Non-Condon vibronic coupling of coherent molecular vibration in MEH-PPV induced by a visible few-cycle pulse laser

2009 New J. Phys. 11 013048

(http://iopscience.iop.org/1367-2630/11/1/013048)

New Journal of Physics
The open-access journal for physics

Non-Condon vibronic coupling of coherent molecular vibration in MEH-PPV induced by a visible few-cycle pulse laser

Takayoshi Kobayashi[1,2,3,4,5], **Jun Zhang**[1] **and Zhuan Wang**[1,2]

[1] Department of Applied Physics and Chemistry and Institute for Laser Science, University of Electro-Communications, 1-5-1 Chofugaoka, Chofu, Tokyo 182-8585, Japan

[2] JST, ICORP, Ultrashort Pulse Laser Project, 4-1-8 Honcho, Kawaguchi, Saitama, Japan

[3] Department of Electrophysics, National Chiao Tung University, 1001 Ta Hsueh Road, Hsin-Chu 3005, Taiwan

[4] Institute of Laser Engineering, Osaka University, 2–6 Yamada-Oka, Suita, Osaka 565-0971, Japan

E-mail: kobayashi@ils.uec.ac.jp

New Journal of Physics **11** (2009) 013048 (14pp)
Received 5 August 2008
Published 26 January 2009
Online at http://www.njp.org/
doi:10.1088/1367-2630/11/1/013048

Abstract. Vibrational real-time spectra of poly-[2-methoxy-5-(2′-ethyl-hexyloxy)-*p*-phenylene vinylene] (MEH-PPV) were measured in a 5 fs pump–probe experiment simultaneously at 128 probe wavelengths with a multi-channel detection system. The spectral dependence of the coherent vibrational amplitudes obtained from the Fourier transform (FT) on the probe wavelength detected was found to be given by the sum of the ground-state absorption spectrum and its first and second derivatives. This indicates that the change of the transition probability caused by a wave packet motion can be explained as induced by both the non-Condon effect (non-Condon (NC) mechanism) and the time-dependent Franck–Condon factor (Frank-Condon (FC) mechanism). The FC mechanism can contribute to the first and second derivatives' dependence. On the other hand, the NC mechanism is dominant in the zeroth-order derivative. This result proves that the 1^1B_u exciton is strongly coupled with the excited ^1A_g state, which is known to be essential in third-order optical nonlinearity. The amounts of shift of the absorption peaks and changes in the bandwidth due to

[5] Author to whom any correspondence should be addressed.

the wave packet motions were determined for the four most prominent modes in the FT power spectra. The shift due to the FC mechanism was about 1.3–1.1% of the peak transition energy and the broadening of the vibronic transition due to the NC mechanism was about 8.0–7.6% of the bandwidth for the four modes. A novel ultrafast optical switch utilizing the modulation of electronic transition probability by molecular vibration through vibronic coupling and the interference of the wave packets is proposed.

Contents

1. Introduction

The ability to tailor morphological, mechanical, electrical and optical properties by chemical modification makes conjugated polymers remarkable materials. These properties are very useful for the modification of electrooptical (EO) and optoelectrical (OE) properties, which are of vital importance for various applications, such as electroluminescent devices, nonlinear optical devices and field-effect transistors [1]–[14]. Both the optical and electrical properties of the materials can be chemically controlled by the addition of side chains onto the main chain of a conjugated polymer using synthetic methods. One of the most promising conjugated polymers belongs to the poly(*p*-phenylene vinylene) (PPV) family. Among PPVs, the most extensively studied is poly-[2-methoxy-5-(2′-ethyl-hexyloxy)-*p*-phenylene vinylene] (MEH-PPV) because of its high solubility in common solvents and high electroluminescence efficiency.

The mechanism of the efficient luminescence in MEH-PPV has been well described and characterized in terms of stably bound electron–hole excitons [15]–[17]. The symmetries of excitons in conducting polymers with inversion symmetry are classified as even (A_g) or odd (B_u) parity. It has been verified theoretically and experimentally that such A_g states are located above the lowest 1^1B_u state in several derivatives of PPV [6, 10, 15, 16]. A detailed understanding of the mechanism and dynamics of photoexcitations and vibronic coupling in MEH-PPV is highly desirable because of its relevance to radiationless relaxation, which determines the luminescence efficiency. To clarify the mechanism of nonradiative processes, it is most straightforward to time-resolve the processes using a pulsed laser with sufficiently short pulse duration [18]–[20]. Ultrashort pulses are even more advantageous, because pulses shorter than the characteristic relaxation time of the exciton state can provide detailed insights into the dynamics associated with the excitonic relaxation processes. Furthermore, the vibrational dynamics can also be studied directly by real-time vibrational spectroscopy through the electronic transition probability modulation induced by the instantaneous structural change of

molecules. The modulation of the transition intensity is through vibronic coupling. Therefore, the observation of real-time vibrational dynamics by pump–probe experiment can provide information on vibronic coupling mechanisms through the study of the probe wavelength dependence of the vibrational amplitude. It can also provide information on structural change. It can thus reveal the mechanism of the radiationless process, which is the conversion process of electronic energy into vibrational energy. Therefore, it is necessary to clarify the mechanism of vibronic coupling for the study of radiationless relaxation mechanisms, which are of essential importance for determining the efficiency of luminescence. In spite of the importance of understanding the mechanism of vibronic coupling, few studies have been conducted on MEH-PPV; hence, the study of vibronic coupling in this system is highly compelling.

Vibronic coupling also determines the size of the third-order nonlinear optical properties through the excitation-induced structural change due to spontaneous geometrical relaxation in a one-dimensional system [21]. This relaxation induces spectral changes in absorption, fluorescence and gain, all of which originate from the imaginary part of the third-order nonlinear susceptibility, whereas the real part of the third-order susceptibility induces a phase change. The structural change after the geometrical relaxation can be studied using the time dependence of instantaneous vibrational frequencies of the photoexcited molecule by comparing the observed frequencies with the abundant data on vibrational frequencies of a large number of molecules.

In general, the Condon approximation is a good approximation in many organic molecules. In the case where the approximation is well satisfied, two slightly different mechanisms for vibronic coupling relevant to the electronic (vibronic) transitions are generally discussed. The first one is due to the shift in the potential minima between the ground state and the excited state. This mechanism is due to the time-dependent Franck–Condon overlap oscillating with a vibrational mode frequency. The second is the difference in the curvature of the potential curves between the ground state and the excited state. This mechanism is due to the Herzberg–Teller (HT) effect. No studies on the HT effect in MEH-PPV or other members of the PPV polymer family were found in the literature apart from the proposal of an intermolecular HT effect [22].

Furthermore, there is the possibility of deviation from the Condon approximation. In this case, time-dependent Franck-Condon overlap and the HT effect are not enough to explain the vibronic mechanism. In the present study, we discussed the Condon approximation and the deviation from it with a simple model and studied the vibronic coupling mechanism in the MEH-PPV after photoexcitation.

Several research studies on MEH-PPV using ultrashort laser pulses with pulse durations from several tens to 100 fs have been reported [23]–[25]. However, no study has yet been reported on coherent molecular vibration induced by impulsive excitation with a sufficiently short pulse.

In this paper, we report the results of real-time vibrational spectroscopy for MEH-PPV excited by a laser pulse of 5.7 fs duration, which is short enough to impulsively excite several vibrations of the molecule, and we show that the non-Condon effect is substantially large in the vibronic coupling mechanism.

2. Experiment

A noncollinear optical parametric amplifier (NOPA) [26]–[29] was used as a light source for the pump–probe experiment as described in our previous papers [30]–[32]. Several features of the system are described below. The pump source of this system was a commercial regenerative

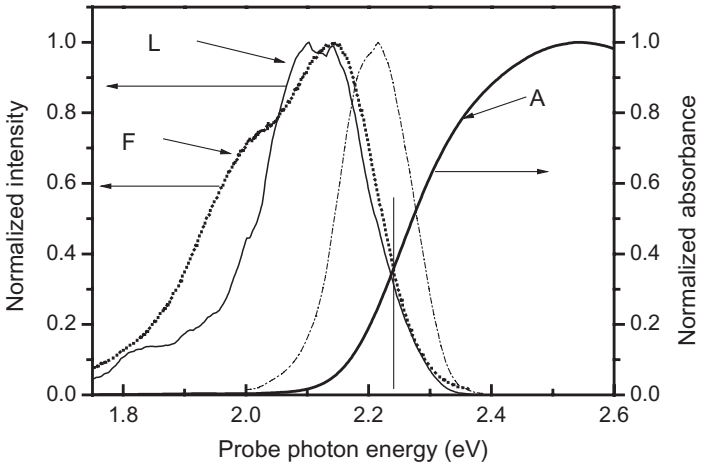

Figure 1. Stationary absorption spectrum (A, thick solid line), laser spectrum (L, thin solid line), absorbed laser spectrum (A–L, calculated from A and L) and fluorescence (F, dotted line). The straight line in the figure shows the photon energy of the 0–0 transition, which is given by the crossing point of the normalized absorption and fluorescence spectra.

amplifier (Spitfire; Spectra Physics). Its central wavelength, pulse duration, repetition rate and average output power were 790 nm, 50 fs, 5 kHz and 800 mW, respectively. The output pulse from the NOPA was compressed with an optical pulse compressor composed of a pair of Brewster-cut prisms and a pair of chirped mirrors. The bouncing number of the pulse at the chirped mirror was set at 6. The beam was passed through the prism pair twice near their apexes. The shortest pulse duration was 5.7 fs and covered the spectral range from 520 to 750 nm, within which it carried a nearly constant spectral phase, resulting in nearly Fourier transform (FT)-limited pulses.

The laser pulse was split by two beam splitters. One was used to split the pulse into two and the other was used to compensate the group-velocity dispersion in the former. The pulse energies of the pump and probe were about 35 and 5 nJ, respectively. The pulse broadening due to the transmission through the air and some optical components was controlled by fine-tuning of the distance between the above-mentioned prism pair. A 128-channel lock-in amplifier was used as a phase-sensitive broad band detector [30] to collect the pump–probe signals. In the present experiment, the modulation frequency was set at 2.5 kHz.

Absorption and fluorescence spectra were measured with an absorption spectrometer (model UV-3101PC; Shimadzu) and a fluorophotometer (model F-4500; Hitachi), respectively. Chloroform solutions of MEH-PPV were spin-coated onto quartz plates to form 0.5–1.0 μm thick films. All the experiments were performed at room temperature (293 $\pm$ 1 K).

3. Results and discussion

3.1. Fourier power spectra of real-time traces

Figure 1 shows the stationary absorption and fluorescence spectra of the thin film sample and the spectrum of the 5.7 fs pulsed laser. The laser spectrum may overlap the 0–0 and 0–1

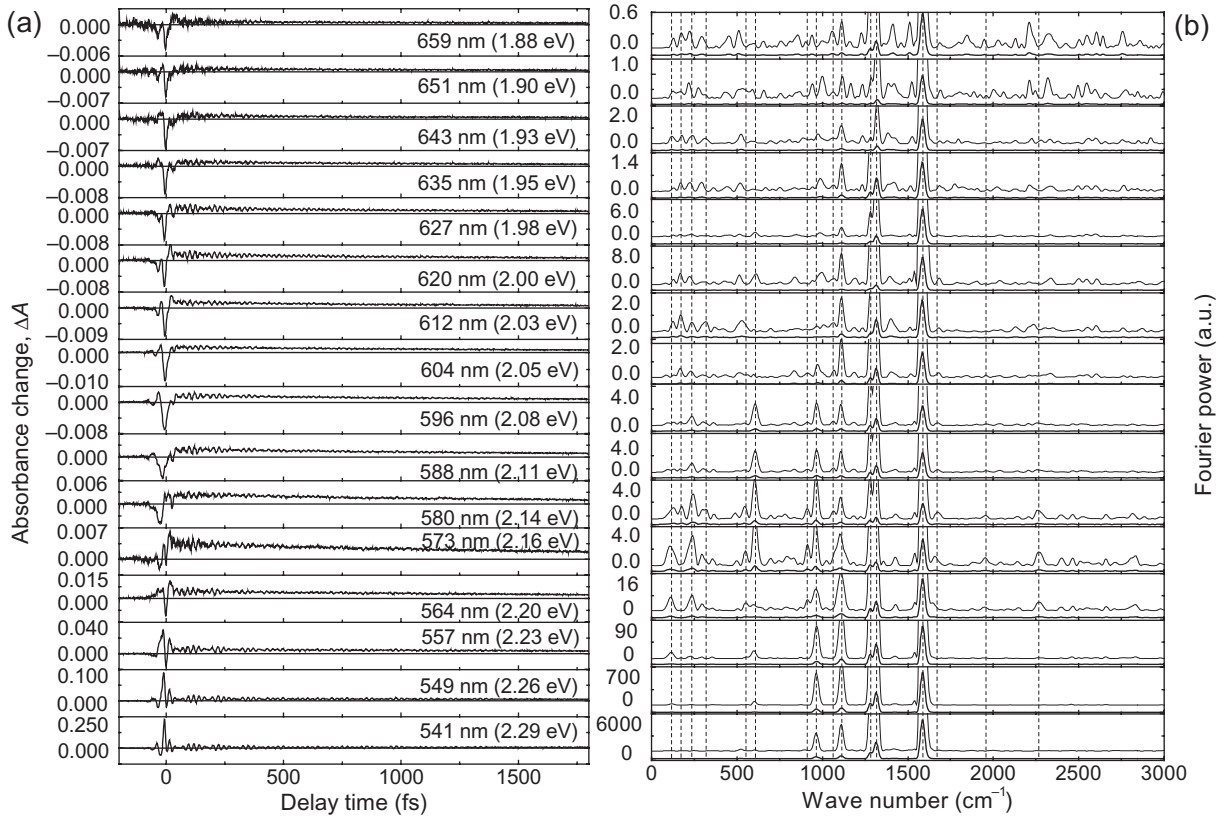

Figure 2. (a) The change in the absorbance as a function of pump–probe delay time at 16 different probe wavelengths (photon energies) and (b) FFT power spectra (solid thick lines) of traces as shown in (a). The dashed lines mark the reproducible peaks.

vibronic transitions in the absorption spectrum for the modes with frequencies lower than 800 cm^{-1} (0.10 eV) assuming that the 0–0 transition is located at about 2.24 eV. The energy of the 0–0 transition was determined from the crossing point of the normalized absorption and fluorescence spectra. From the laser spectrum and sample absorption spectrum, the absorbed laser spectrum was calculated, as shown in figure 1. The spectrum has two features: (1) a peak at 2.216 eV, which is lower than the 0–0 transition energy of 2.24 eV, and (2) asymmetry with a more extended tail toward lower energies than toward higher energies. Therefore, it can be concluded that the contribution of the 0–0 transition dominates that of the 0–1 transition in the absorption.

Figures 2(a) and (b) show the real-time traces of the pump–probe experiment and the Fourier power spectra of the traces for 16 different probe photon energies (wavelengths), respectively. The time range for the fast Fourier transform (FFT) calculation was from 50 to 1800 fs. The time range did not start at 0 fs to avoid the effect of interference between the probe pulse and scattered pump pulse. Even though the pulse duration is 5.7 fs, the spatial coherence is very high and a multiply scattered pump pulse exists for up to a few microns, which is the thickness of the sample film corresponding to a pulse duration of 10–20 fs. Therefore, such an

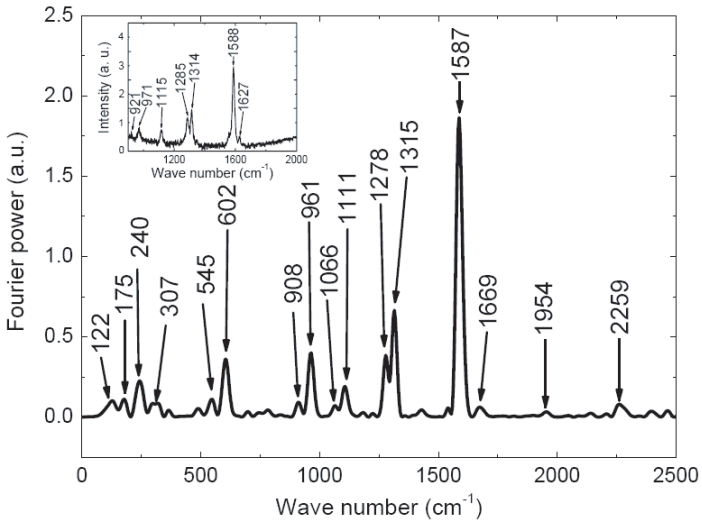

Figure 3. FFT power spectrum of the vibrational real-time spectrum probed at 580 nm. The inset shows the RS spectrum of MEH-PPV excited at 632.8 nm.

interference can take place even for a delay time of 20 fs, and hence it was necessary to use probe delay times longer than 50 fs to ensure that this coherent effect did not occur.

The Fourier power spectrum at 2.14 eV (580 nm) is shown on an expanded scale in figure 3 as an example. The frequencies of the intense peaks in the spectrum are 122, 175, 240, 307, 545, 602, 908, 961, 1066, 1111, 1278, 1315, 1587, 1669, 1954 and 2259 cm^{-1}. Possible errors in the determination of the frequencies are about $\pm 8\,cm^{-1}$. The error is mainly due to the finite probe delay time length. They were also found at other probe photon energies (wavelengths) as indicated by dashed lines in figure 2(b).

The vibrational modes that appear in the pump–probe experiment have the same selection rule as that of Raman scattering. The Raman spectrum of the sample using an He–Ne laser is shown in the inset of figure 3. There are common lines with nearly the same frequencies in the Raman spectrum and the Fourier power spectrum of the real-time vibration. From higher frequencies, the lines are located at 1588 cm^{-1} (Raman scattering, hereafter referred to as RS)–1587 cm^{-1} (real-time vibration, hereafter referred to as RT), 1314 cm^{-1} (RS)–1315 cm^{-1} (RT), 1285 cm^{-1} (RS)–1278 cm^{-1} (RT), 1115 cm^{-1} (RS)–1111 cm^{-1} (RT) and 971 cm^{-1} (RS)–961 cm^{-1} (RT).

We used the assignment of Raman and infrared spectra of PPV in the literature [33] to assign the modes observed in the present study. The peaks at 1587, 1315, 1278 and 961 cm^{-1} were attributed to ring stretching and vinyl C=C stretching, vinyl CH in-plane bending, ring stretching and CH out-of-plane bending modes, respectively [33].

A two-dimensional plot of Fourier amplitudes against the molecular vibration frequency and probe photon energy (wavelength) is presented in figure 4(a). This figure shows that Fourier amplitudes increase very rapidly with the photon energy (wavelength) in the range from about 2.20 eV (563 nm) to 2.39 eV (519 nm). This is clearly seen in figure 4(b), which shows the example of the 1587 cm^{-1} mode. The probe photon energy dependence of vibrational amplitudes of the modes was analyzed to clarify the mechanism of the modulation of electronic transition probability.

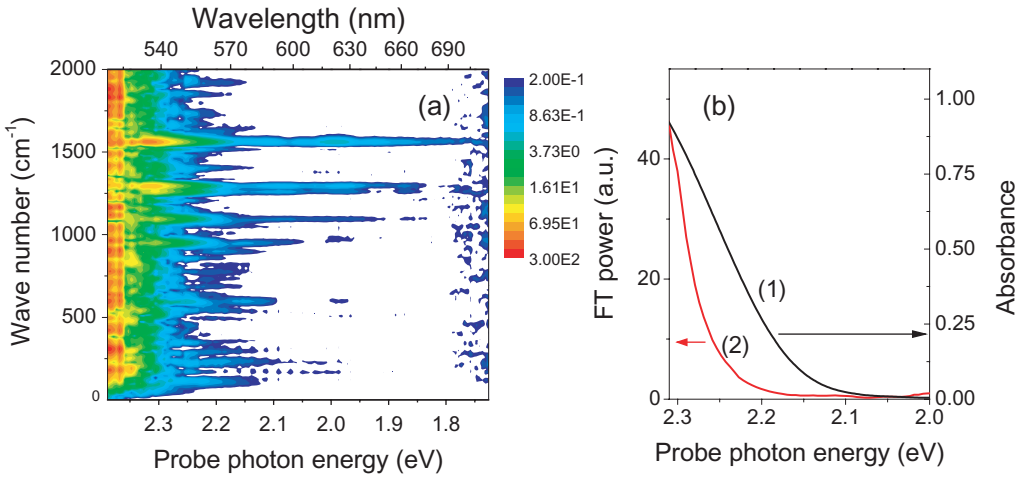

Figure 4. (a) Contour map of the Fourier amplitude of oscillation in the absorbance change plotted against the probe photon energy (wavelength) and vibrational frequency. The Fourier power is indicated on the logarithmic scale with a step of 1.44. (b) The probe photon energy dependence of ground-state absorption intensity (line 1) and FT power of 1587 cm^{-1} (line 2).

3.2. Potential curves and spectral change due to wave packet motion

To clarify the physical significance of the spectral dependence of the Fourier amplitude, the modulation of transition probability is discussed using a very simple model with two harmonic potential curves belonging to the ground state and the excited state. In this case, the two relevant bands of the ground state (α) and the excited state (β) can be described by using simple parabolic potential curves given by the following equations:

$$U_\alpha = AQ^2, \tag{1}$$

$$U_\beta = B(Q - Q_0)^2 + \Delta E. \tag{2}$$

Here, A and B are related to the curvatures of the potential curves, Q is a normal coordinate of a molecular vibration mode, Q_0 is the displacement of the equilibrium and ΔE is the 0–0 transition energy.

There are four typical cases of the minima and curvatures of the two potential curves. (1) There is neither displacement of the minimum (DM) nor curvature change (CC) upon photoexcitation; $Q_0 = 0$, $A = B$. The energy difference between the excited state and the ground state $\Delta U = U_\beta - U_\alpha = \Delta E$ is independent of Q. (2) There is DM but no CC; $Q_0 \neq 0$, $A = B$. In this case, $\Delta U = \Delta E - 2BQQ_0 + BQ_0^2$ is a linear function of Q. (3) There is CC but no DM; $Q_0 = 0$, $A \neq B$. $\Delta U = (B - A)Q^2 + \Delta E$ is the quadratic function of Q without a linear term. (4) There is both DM and CC; $Q_0 \neq 0$, $A \neq B$. In this case, $\Delta U = (B - A)Q^2 - 2BQQ_0 + \Delta E$ is a quadratic function of Q with a linear term.

The absorption spectrum corresponding to the transition between the lower and upper potential curves is given by the energy distribution of $\Delta U(Q)$ with respect to the optical (probe) frequency. We try to relate $\Delta U(Q)$ with the optical probe frequency in the following.

The molecular vibrational motion can be described phenomenologically in a classical model by the following equation:

$$\frac{\mathrm{d}^2 Q}{\mathrm{d}t^2} + \omega_v^2 Q = F. \tag{3}$$

Here, Q is a normal coordinate of a molecular vibration mode with frequency ω_v, and F is the driving force [34, 35]. In transparent media, it has been known for a long time that vibrational coherences rely on coherent (stimulated) RS (CRS) for which $F = \sum_{\mu v} (\chi^{\mathrm{R}}_{\mu v} E_\mu E_v)/2$. Here, $E_{\mu(v)}$ denotes a component of the optical pump field, $\chi^{\mathrm{R}}_{\mu v} \approx \partial \chi^{(1)}_{\mu v}/\partial Q$ is the nonlinear Raman susceptibility and $\chi^{(1)}_{\mu v}$ is the linear susceptibility [35]–[37]. In the case of absorbing materials, for which the electronic transition is resonant with a laser field and/or Stokes (anti-Stokes) field, $\chi^{\mathrm{R}}_{\mu v}$ becomes complex.

In the case of two-potential curves, because the derivative of the susceptibility $\chi^{(1)}$ with respect to the normal coordinate is proportional to the derivative of $\chi^{(1)}$ with respect to optical frequency, $\partial \chi^{(1)}/\partial Q \propto \partial \chi^{(1)}/\partial \omega_v$ is satisfied. Therefore, the probe photon energy dependence of the vibrational amplitude, which is proportional to the Raman susceptibility, can be discussed in terms of the frequency derivative of the linear susceptibility $\chi^{(1)}$. The spectral change induced by the modulation of Q (vibration) by the amount of ΔQ is then given by $(\partial \chi^{(1)}/\partial Q)\Delta Q$, which is proportional to $\partial \chi^{(1)}/\partial \omega$ and hence to the frequency derivative of the absorption spectrum. In case (3), where $\partial \chi^{(1)}/\partial Q$ is zero, the dominant contribution of the spectral change associated with the modulation of Q by an amount of ΔQ is given by the second-order term proportional to $(1/2)(\partial^2 \chi(1)/\partial Q^2)(\Delta Q)^2$. This term is then proportional to $\partial^2 \chi^{(1)}/\partial \omega^2$ in the same way as in the linear case discussed above.

To analyze the data on the absorption spectral range of MEH-PPV, we make four assumptions in the following discussion. They are as follows: (a) Initially, there is no population on the vibrational levels with quantum numbers larger than $v = 0$ in the electronic ground state, because the mode frequency is sufficiently high for the level not to be populated at the experimental temperature. This is satisfied for the four modes with frequencies of 961, 1278, 1315 and 1587 cm^{-1}; the last of these modes is discussed in section 3.3. (b) A wave packet is generated only in the ground state with an ultrashort pulse through the stimulated Raman process. From the absorbed laser spectrum shown in figure 1, it was calculated that only about 1.8% of the absorbed photons were used for the 0–1 transition for the mode with a frequency of 961 cm^{-1}. The fraction of the 0–1 transition for the other three modes was estimated to be much less than 1%. Therefore, the pump laser did not excite the 0–1 vibronic level sufficiently to form the excited wave packet via simultaneous coherent excitation of 0–0 and 0–1 (and higher) vibronic levels. (c) The amplitude of the wave-packet motion is small enough for the change in the absorbance difference ΔA by $\delta \Delta A$ to be proportional to the vibrational amplitude. This is a reasonable assumption because a small Huang–Rhys factor was determined, namely 0.51 [38]. (d) It is assumed at first that the Condon approximation is satisfied. The deviation from the Condon approximation is discussed later.

The four different cases relevant to the above potential features are as follows. (1′) There is generation of a vibrational eigenstate without any wave packet motion. (2′) There is generation of a wave packet in the ground state, which starts to displace along the potential curve. The probe frequency dependence of the vibrational amplitude is given by the first derivative $A'(\omega)$ of the ground-state absorption ($A(\omega)$) spectrum. This is due to the time-dependent Franck–Condon factor associated with the wave packet motion [39]. (3′) There is generation of a wave packet

in the ground state, which starts to breathe. The probe frequency dependence of the vibrational amplitude is given by the second derivative ($A''(\omega)$) of the ground-state absorption ($A(\omega)$). (4′) There is generation of a wave packet in the ground state, which starts to displace along the potential curve and breathe at the same time. The probe frequency dependence of the spectral change due to the wave packet motion is given by the sum of the first and second derivatives of the ground-state absorption.

In general, the Condon approximation is a good approximation in many organic molecules. Also, there is always a finite Huang–Rhys factor inducing wave packet motion due to displacement, resulting in a finite Stokes shift except in the extreme case of no potential displacement as in J-aggregates [39, 40]. Therefore, case (2) can be found in most cases. In this case the probe wavelength dependence is given by the first derivative. If the Huang–Rhys factor is not substantially large (<2), then case (3) will be realized. In this case the probe wavelength dependence is given by the second derivative.

In the above discussion, for all of the cases it was assumed that the Condon approximation is satisfied because the integrated intensity of the absorbance change covering the relevant electronic state does not change during the wave packet motion. The deviation from the Condon approximation can then be introduced by taking into account another electronic state (a third state), which is radiatively coupled to the two states between which transition intensity is being monitored. In the present case, the two corresponding states are the ground state and the lowest excited state. In the case of non-Condon (NC) type mechanism, the effect of modulation of the transition probability discussed in the above four cases can be modified in the following ways. In cases (2″), (3″) and (4″), there will be the extra contributions from the ground-state absorption ($A(\omega)$) to the probe wavelength dependence of the vibrational amplitude.

3.3. Vibronic coupling mechanisms

Following the above simple general discussion, vibrational Fourier amplitudes over 128 different photon energies (wavelengths) measured at the same time in the present study were analyzed as follows.

The probe photon energy dependences of the four most intense modes (961, 1278, 1315 and 1587 cm^{-1}) have the common feature that the signal intensity increases with an increase in the probe photon energy. The amplitudes of all four modes have very large values in the spectral range of 2.18–2.28 eV, which indicates that the transition probability change due to the deformation induced by molecular vibration is large in this spectral range. In this spectral range, they can be well reproduced by the combination of the zeroth, first and second derivatives of the absorption spectrum as with the expression $aA(\omega) + bA'(\omega) + cA''(\omega)$). Here, a, b and c represent the weight factors. The results are shown in figures 5(a)–(d). The contributions of the zeroth, first and second derivatives are separated as a function of photon energy in figures 5 (a′)–(d′).

As shown in figures 5(a′)–(d′), the contribution of the FT amplitude of the vibrational modes from the zeroth derivative of the ground-state absorption spectrum is negligible, especially small in the high photon energy side. Therefore, the intense signal observed in the ground-state absorption spectral region can be explained by the NC mechanism as discussed in section 3.2. The non-Condon effect is due to the strongly allowed electronic state(s) existing at higher energies than that of the relevant state. Several theoretical and experimental papers have verified that such A_g-symmetry states are located above the 1^1B_u state [15, 41, 42].

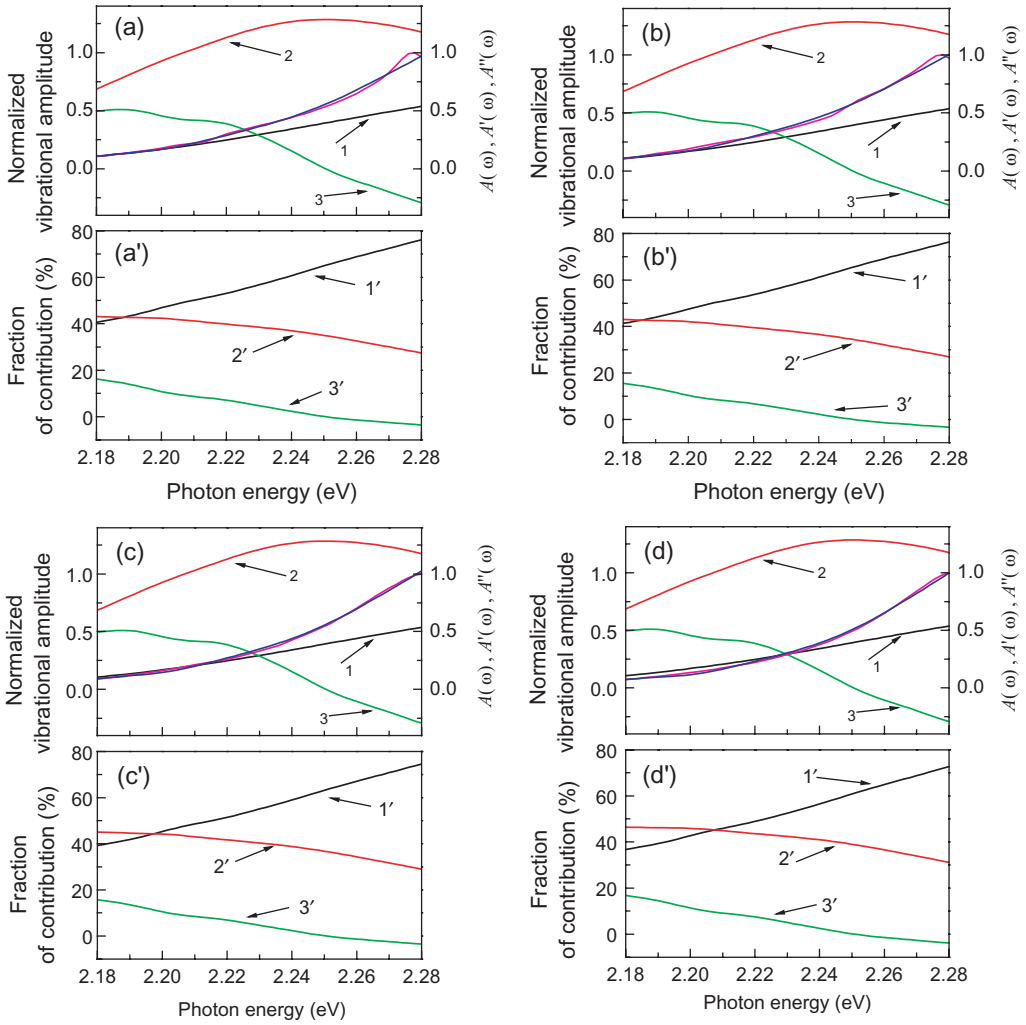

Figure 5. (a) (a′), (b) (b′), (c) (c′) and (c) (d′) correspond to 961, 1278, 1315 and 1587 cm^{-1}, respectively. (a)–(d) Probe photon energy dependence of the normalized vibrational amplitude, absorbance and its derivatives. Lines 1, 2 and 3 represent the zeroth, first and second derivatives ($A(\omega)$, $A'(\omega)$ and $A''(\omega)$) of the ground-state absorption, respectively. $A(\omega)$, $A'(\omega)$ and $A''(\omega)$ are in units of OD (optical density), OD s^2 rad^{-1} $\times 10^{13}$ and OD s rad^{-2} $\times 10^{26}$. The blue line represents the combination of these three elements with the expression $aA(\omega) + bA'(\omega) + cA''(\omega)$), where a, b and c are the weight factors; the pink line is the mode amplitude from FT. (a′)–(d′) The fraction of contribution from the zeroth (line 1′), first (line 2′) and second (line 3′) derivatives of the ground-state absorption spectrum to the vibrational mode.

They are called m^1A_g and n^1A_g states and greatly contribute to the third-order optical non-linearity [41, 42].

In table 1, the calculated weight factors a, b and c, in the FT amplitude fitting the equation $aA(\omega) + bA'(\omega) + cA''(\omega)$, are listed for the four modes studied. All the modes have positive a and c and negative b. The positive as suggest the mechanism of the deviation from the Condon

Table 1. The weight factors a, b and c in the FT amplitude fitting the expression $aA(\omega)+bA'(\omega)+cA''(\omega)$. a, b and c are the calculated weight factors. The ratios $|b/a|$ and $|c/a|$ are also listed.

Mode (cm^{-1})	a	b	$\lvert b/a\rvert$	c	$\lvert c/a\rvert$
1587	3.58	−0.70	0.2	0.35	0.10
1315	3.38	−0.60	0.18	0.29	0.09
1278	2.99	−0.46	0.15	0.21	0.07
961	2.98	−0.48	0.16	0.24	0.08

Table 2. Electronic transition peak shift, fraction of the shifts, electronic transition band broadening and fraction of the broadening corresponding to the modes with frequencies of 1587, 1315, 1278 and 961 cm^{-1}.

Mode (cm^{-1})	Electronic transition peak shift (cm^{-1})	Fraction of the shift (%)	Electronic transition band broadening (cm^{-1})	Fraction of the broadening (%)
1587	278	1.3	489	8.0
1315	257	1.3	480	7.8
1278	257	1.3	480	7.8
961	223	1.1	470	7.6

approximation. In the vibronic coupling of these four modes, the intensity is borrowed from higher excited state(s), which have higher oscillator strength of transition from the ground state than that of the lowest excited state [43]. The negative bs mean that the transition energy shifts to higher transition energy for all of the vibrational modes. This is very reasonable if we consider the relation of the potential energy difference given by $\Delta U = \Delta E - 2BQQ_0 + BQ_0^2$ and $\partial\chi^{(1)}/\partial Q \propto \partial\chi^{(1)}/\partial\omega_v$. These equations mean that the wave packet motion is always in the direction of the smaller transition energy. The positive c indicates that the mode softening takes place for all the four modes. This is due to the fact that the three modes with frequencies of 1587, 1315 and 1278 cm^{-1} have contributions to C=C stretching the spring constant of which becomes weaker upon π–π^* excitation as expected. By comparing the ratios $|b/a|$ and $|c/a|$ among the four modes, we can conclude that the effects of potential shift and broadening (softening) are largest in the 1587 cm^{-1} mode. In other words, the relative amount of deviation from the Condon approximation is smallest in the highest frequency 1587 cm^{-1} mode among the four modes, which couple strongly to the $S_1 \leftarrow S_0$ transition.

From the data of the contribution of $A(\omega)$, $A'(\omega)$ and $A''(\omega)$, the energy shift ($A'(\omega)$) and broadening ($A''(\omega)$) were estimated to be about 0.034 eV (278 cm^{-1}) and about 0.061 eV (489 cm^{-1}), respectively, at 1587 cm^{-1}. The shift corresponds to 1.3% of the electronic transition energy (2.541 eV) and the broadening corresponds to 8% of the width (full-width at half-maximum (FWHM)) of the relevant transition (0.759 eV) for the 1587 cm^{-1} mode. The electronic transition energy shifts and broadenings for the four modes including those for the 1587 cm^{-1} mode are listed in table 2.

The changes in the peak photon energy and bandwidth of the relevant vibronic transitions contribute to the ultrafast optical nonlinearity. The nonlinearity may be able to be used in optical logic operation by applying two pulses in succession to produce constructive and/or destructive interference between the two wave packets generated by the two optical ultrashort pulses. For example, in the case of the second pulse reaching the polymer system after a time period equal to the half integer multiple of the vibrational period, this 'vibronic' nonlinearity is turned off, thus realizing ultrafast nonlinear optical switching. This switching can be as fast as a few tens of femtoseconds.

Another possible mechanism is the anharmonicity of potential curves. If the potential shifts between the ground state and the excited state with the curvature stay constant, the transition energy ω is proportional to Q, whereas if there is no shift but a difference in the mode frequency, then ω is proportional to Q^2. If anharmonicity is included, then the transition energy can be given by $AQ + BQ^2 + CQ^3 + \Lambda$. A similar relation to the previous one can be given as $\partial^2\chi(\omega)/\partial\omega^2 \propto \partial^2\chi(\omega)/\partial Q^2$. Therefore, it is possibile that anharmonicity contributes to the special dependence in the shape of the second derivative of the absorption spectrum. However, in the present experiment, the active vibrational modes are in the range of 950–1600 cm^{-1} and the maximum bandwidth of the laser spectrum is about 5000 cm^{-1}. With the RS, at the most $v = 5$ of the vibronic level in the ground state can be excited, which shows very low probability that the anharmonicity contributes. Therefore, for the present study, it is safe to give the conclusion that the intense signal observed in the ground-state absorption spectral region can be explained by the NC mechanism.

4. Conclusion

A coherent molecular vibration in MEH-PPV was studied using extremely short laser pulses and a system for detecting 128 different wavelengths. An investigation was conducted on the probe photon energy dependences of the vibrational amplitudes of the four most prominent modes with frequencies of 961, 1287, 1315 and 1587 cm^{-1}. It was found that all the amplitudes could be reproduced by the combination of functions of optical frequency given by the ground-state absorption spectrum ($A(\omega)$), and its first ($A'(\omega)$) and second ($A''(\omega)$) derivatives with respect to the frequency. From the spectral dependence of the molecular vibrational amplitudes of these modes, the frequency dependences of the contributions of the mechanisms were obtained. It was also found that the integrated area of the spectral change in the lowest electronic transition range has a large positive value. From these results, it is concluded that the modulation of the transition probability change in the MEH-PPV transient absorption by molecular vibration through vibronic coupling is induced substantially by the non-Condon effect together with the time-dependent Franck-Condon factor.

Acknowledgments

We acknowledge Professor Eiji Tokunaga (Physics Department, Tokyo University of Science) for his help in the measurement of the Raman spectrum. This work was partly supported by the 21st Century COE program on 'Coherent Optical Science' and partly supported by a grant from the Ministry of Education (MOE) of Taiwan under the ATU Program at the National Chiao Tung University. A part of this work was performed under a joint research project of the Institute of Laser Engineering, Osaka University, under contract number B1-27.

References

[1] Sáfar G A M, Oliveira F A C, Cury L A, Righi A, Barbosa P L M, Dieudonné P and Lameiras F S 2006 *J. Appl. Polym. Sci.* **102** 5620
[2] Friend R H *et al* 1999 *Nature* **397** 121
[3] Hide F, Díaz-García M A, Schwartz B J and Heeger A J 1997 *J. Acc. Chem. Res.* **30** 4301
[4] Rothberg L J and Lovinger A J 1996 *J. Mater. Res.* **11** 3174
[5] Kobayashi T 1989 *Nonlinear Optics of Organics and Semiconductors* (Berlin: Springer)
[6] Etemad S and Soos Z G 1991 *Spectroscopy of Advanced Materials* ed R J H Clark and R E Hester (New York: Wiley)
[7] Mahrt R F, Pauck T, Lemmer U, Sieger U, Hopmeier M, Hennig R, Bässler H and Göbel E O 1996 *Phys. Rev.* B **54** 1759
[8] Heeger, Kivelson S, Schrieffer J R and Su W-P 1988 *Rev. Mod. Phys.* **60** 781
[9] Burn P L, Holmes A B, Kraft A, Bradley D D C, Brown A R, Friend R H and Gymer R W 1992 *Nature* **356** 47
[10] Hayes G R, Samuel I D W and Phillips R T 1995 *Phys. Rev.* B **52** R11569
[11] Robert R B, Richard W Z and Raymond K K 1999 *Appl. Opt.* **38** 5181
[12] Matthew W, Guangzhou C, Yanyun Z, Brian G B and Robert T D 2007 *Appl. Opt.* **46** 3177
[13] Park B, Paoprasert P, In I, Zwickey J, Colavita P E, Hamers R J, Gopalan P and Evans P G 2007 *Adv. Mater.* **19** 4353
[14] Gershenson M E, Podzorov V and Morpurgo A F 2006 *Rev. Mod. Phys.* **78** 973
[15] Liess M, Jeglinski S, Vardeny Z V, Ozaki M, Yoshino K, Ding Y and Barton T 1997 *Phys. Rev.* B **56** 15712
[16] Abe S 1989 *J. Phys. Soc. Japan* **58** 62
[17] Ogawa T and Takagahara T 1991 *Phys. Rev.* B **44** 8138
[18] Schryver F C, Feyter S and Schweitzer G (ed) 2001 *Femtochemistry* (Weinheim: Wiley-VCH)
[19] Douhal A and Santamaria J (ed) 2001 *Femtochemistry and Femtobiology* (Singapore: World Scientific)
[20] Castleman A W Jr and Kimble M L (ed) 2006 *Femtochemistry VII: Fundamental Ultrafast Processes in Chemistry, Physics, and Biology* (Amsterdam: Elsevier)
[21] Kobayashi T, Yoshizawa M, Stamm U, Taiji M and Hasegawa M 1990 *J. Opt. Soc. Am.* B **7** 1558
[22] Bittner E R and Karabunarliev S 2007 *J. Chem. Phys.* **126** 191102
[23] Hagler T W, Pakbaz K and Heeger A J 1995 *Phys. Rev.* B **51** 14199
[24] Yang X, Dykstra T E and Scholes G D 2005 *Phys. Rev.* B **71** 045203
[25] Ruseckas A and Samuel I D W 2006 *Phys. Status Solidi* c **3** 263
[26] Ruseckas A, Wood P, Samuel I D W, Webster G R, Mitchell W J, Burn P L and Sundström V 2005 *Phys. Rev.* B **72** 115214
[27] Shirakawa A, Sakane I and Kobayashi T 1998 *Opt. Lett.* **23** 1292
[28] Shirakawa A, Sakane I, Takasaka M and Kobayashi T 1999 *Appl. Phys. Lett.* **74** 2268
[29] Baltuska A, Fuji T and Kobayashi T 2002 *Opt. Lett.* **27** 306
[30] Kobayashi T, Saito T and Ohtani H 2001 *Nature* **414** 531
[31] Kobayashi T, Shirakawa A, Matsuzawa H and Nakanishi H 2000 *Chem. Phys. Lett.* **321** 385
[32] Ishii N, Tokunaga E, Adachi S, Kimura T, Matsuda H and Kobayashi T 2004 *Phys. Rev.* A **70** 023811
[33] Honda K, Furukawa Y and Nishide H 2006 *Vib. Spectrosc.* **40** 149
[34] Garrett G A, Albrecht T F, Whitaker J F and Merlin R 1996 *Phys. Rev. Lett.* **77** 3661
[35] Ruhman S, Joly A G and Nelson K A 1988 *IEEE J. Quantum Electron.* **24** 460
[36] Kütt W A, Albrecht W and Kurz H 1992 *IEEE J. Quantum Electron.* **28** 2434
[37] Shen Y R and Bloembergen N 1965 *Phys. Rev.* A **137** 1787
[38] Shanyu Q, Feng T, Zheng X, Lei Q, Ting Z, Deang L, Yanbin H, Yongsheng W and Xurong X 2006 *Mater. Lett.* **60** 1134

[39] Kobayashi T, Wang Z and Otsubo T 2007 *J. Phys. Chem.* A **111** 12985
[40] Kobayashi T (ed) 1996 *J-aggregates* (River Edge, NJ: World Scientific)
[41] Mazumdar S and Guo F 1994 *J. Chem. Phys.* **100** 1665
[42] Guo F, Guo D and Mazumdar S 1994 *Phys. Rev.* B **49** 10102
[43] Kano H, Santio T and Kobayashi T 2001 *J. Phys. Chem.* B **105** 413